AIP Publishing Applied Physics Letters ACCEPTED MANUSCRIPT
This is the author's peer reviewed, accepted manuscript. However, the online version of record will be different from this version once it has been copyedited and typeset.
PLEASE CITE THIS ARTICLE AS DOI: 10.1063/5.0215146

Pinch-Off Driven Near-ideal Output Characteristics of n-Ga_2O_3/p-GaN Light Effect Transistor for UV Photonics

Arnab Mondal[1], Manoj Kumar Yadav[1], Arpit Nandi[1], Shiv Kumar Bishnoi[2], Indraneel Sanyal[3], Satinder Sharma[1], Jen-Inn Chyi[4] and Ankush Bag[2,5]

AFFILIATIONS

[1] School of Computing and Electrical Engineering, Indian Institute of Technology Mandi, Mandi 175005, India
[2] Department of Electronics and Electrical Engineering, Indian Institute of Technology Guwahati 781039, India
[3] Centre for Device Thermography and Reliability, University of Bristol, United Kingdom.
[4] Department of Electrical Engineering, National Central University, Taoyuan 32001, Taiwan, R.O.C.
[5] Centre for Nanotechnology, Indian Institute of Technology Guwahati 781039, India
Corresponding Author: Ankush Bag (bag.ankush@gmail.com)

ABSTRACT

Gallium Oxide (Ga_2O_3) based phototransistor can be used as a switch and an amplifier in typical digital and analog UV photonic applications, respectively. The light detection capability in Ga_2O_3 is very high, but these phototransistors suffer from poor drain current saturation with bias. Further, the transistor switching action generally necessitates a gate terminal voltage, where a faulty gate power supply can lead to a high current flow in the transistor and subsequently damage the control driver circuit. An alternative is a two-terminal device with pure optical coupling at gate terminal, termed as a light-effect transistor (LET). The LET has the FET-like current-voltage output characteristics, the controlling mode is light instead of voltage, and being a two-terminal device, the fabrication processes are straightforward and cost-effective in contrast to traditional FET. The fabricated LET device comprised an n-Ga_2O_3/p-GaN heterojunction with a planar metal-semiconductor-metal structure. This unique device can operate in two modes, linear (photodetector) within 1-2.5 V, and saturation (depletion width modulated light effect transistor (DM-LET)) within 2.5-5 V. Under the DM-LET mode, the structure exhibits transistor-like action, the drain current saturates with the variation in drain voltage and is only controlled by the change in optical intensity. The transistor-like action has been attributed to the pinch-off effect near the drain electrode due to modulation in the heterojunction depletion width and has been explained using detailed numerical simulation. Such devices have the potential to be used in UV photonic integrated circuits and UV-non-line-of-sight (NLOS) communication technologies.

In today's fast-progressing world, photonic integrated circuits (PICs) and non-line-of-sight (NLOS) communication play an important role in processing and accessing vast information. A UV-NLOS can establish short-range optical data communication and UV-PIC can process the information efficiently [1–3]. However, the technology must be working in the UV region with high gain to reduce any possible background noises. In this regard, Ga_2O_3 has emerged to be a potential semiconductor that can be used in these UV-NLOS and PIC technologies as well as in flame detection, water purification, ozone leakage detection, and missile detection [4]. Having five different phases (α, β, γ, δ, and ε) with β being the most stable one, Ga_2O_3 has a typical ultra-wide bandgap of ~4.8 eV along with a high photoconductive gain. Researchers have shown Ga_2O_3 as an excellent semiconductor for UV solar-blind photodetectors with responsivity even exceeding 10^3 A/W for the conventional two-terminal photodetectors [5,6] and can be further boosted to about 10^7A/W with Ga_2O_3 based phototransistors [7–14]. Such phototransistors are conventional field effect transistors (FET) having source (S), drain (D) and gate (G) terminals and the ability to detect light. The S-D conductivity is modulated to switch ON and OFF the transistor by applying a voltage on the G-terminal. A UV illumination on the device generates additional electron-hole pairs on the S-D channel, increasing the overall current. One of the advantages of the phototransistor is reducing the dark current by applying voltage in the G-terminal, thus, improving the overall light detection performance. Moreover, the phototransistor can also be used as an optoelectronic logic gate as demonstrated by Ji *et al.* [15]. However, the major disadvantages with phototransistors are the inferior drain current (I_D) saturation with drain bias (V_{DS}) or the non-ideal output characteristics under illumination [8,16,17]. The I_D saturation is essential to achieve high output resistance which eventually helps to achieve better transistor performance in both analog and digital applications. Additional complications also arise such as gate fabrication intricacies [18], random doping fluctuations [19] and poor response speed due to gate capacitance. Further, switching of the FET pertains through the gate terminal voltage, a fault in the gate power supply can lead to a high current flow through the FET ensuing fatal damages in the control driver circuit. This type of phototransistor with both

AIP Publishing Applied Physics Letters ACCEPTED MANUSCRIPT
This is the author's peer reviewed, accepted manuscript. However, the online version of record will be different from this version once it has been copyedited and typeset.
PLEASE CITE THIS ARTICLE AS DOI: 10.1063/5.0215146

bias and illumination in the gate terminal is limited to specific applications only.

An alternative is a light effect transistor (LET), a two-terminal (S-D) optoelectronic device purely controlled by light at gate, can imitate FET-like characteristics and offers function that phototransistors or photodetectors cannot achieve. Marmon *et al* [20]. show that a simple metal-semiconductor-metal (MSM) structure on CdSe nanowires can behave like a LET in the visible range and can be used for optical logic gates and optical amplification due to near-ideal output characteristics. For UV radiation Ga_2O_3 is the suitable material for such LET devices, but in state-of-the-art Schottky or Ohmic MSM Ga_2O_3 photodetectors, the typical pinch-off condition in the current conducting channel required to achieve I_D saturation is absent. Ga_2O_3 p-n heterojunction is more promising as the depletion width can be exploited to generate pinch-off conditions in the device under illumination. Ga_2O_3 p-n heterojunction devices have been developed with different materials like p-Si, p-GaN, p-CuO, p-SnO with more emphasis on n-Ga_2O_3/p-GaN heterojunction [21–27]. However, most of the research focuses on the device performance improvement and UV wide-range detection capability. Such heterojunction has also the potential to work as a LET device if the depletion width can be controlled through optical energy rather than electrical energy like in Ga_2O_3 based junction field effect transistors (JFET) [28,29].

To achieve this goal, we fabricate an n-Ga_2O_3/p-GaN heterojunction based LET consisting of an MSM structure on top of n-Ga_2O_3. The metal electrodes serve as either the S or D terminals. The device works as a depletion width modulated light effect transistor (DM-LET). Though a DM-LET has the same MSM structure as a typical photodetector, the uniqueness emanates from its device architecture, operating mechanism and optoelectronic characteristics which distinguish it from typical Ga_2O_3 photodetectors and phototransistors. The DM-LET can imitate the current-voltage characteristics of a conventional FET and offer inimitable functions that are not available in existing photodetectors and phototransistors. The DM-LET shown here relies on a p-n junction structure, where the depletion width modulation and the carrier concentration modulation in S-D channel are controlled solely through optical energy, unlike typical phototransistors where S-D channel's conductivity is controlled through both electrical and optical energy. Again, a simple photodetector cannot be controlled like FET and does not have FET's typical applications like amplification and logic switching due to lack of saturation in I_D. Thus, a DM-LET may behave as a photodetector but a photodetector cannot be LET.

The fabrication of the LET starts with a 500 nm thick Mg-doped GaN grown on a Si wafer using metal-organic chemical vapor deposition technique (MOCVD). The $Al_xGa_{(1-x)}N$ layer below the p-GaN layer acts as a template to grow GaN. With $Al_xGa_{(1-x)}N$ layer and gradient variation of Aluminium (Al) in GaN high quality and very low lattice mismatch GaN layers with low dislocation densities can be obtained on Si wafer. Next, a low-pressure chemical vapor deposition method was employed to grow 180 nm thick Ga_2O_3. The details for the unintentionally doped n-Ga_2O_3 and p-GaN growth method can be found elsewhere [30,31]. The carrier concentration of n-Ga_2O_3 and p-GaN were found to be ≈1.15×10^{15} and ≈2.0×10^{17} /cm^3. The fabricated heterojunction structures were characterized using FESEM, XRD, AFM, and XPS. Reflection electron energy loss spectroscopy (REELS) was employed to evaluate the bandgap of Ga_2O_3. The LET device was fabricated by depositing circular Ti/Au (20/60 nm) electrodes on top of Ga_2O_3 and Ni/Au (20/60 nm) electrode was deposited on p-GaN to verify p-n junction behavior with Ga_2O_3. Post-metallization annealing was done at 450 °C for 90 s to improve the Ohmic behavior. The electrical characterization was performed under dark and illuminated conditions using Keithley 4200 SCS. For photo illumination, a UV lamp (UVP UVLMS-38, Analytikjena, USA) of wavelength λ~254 nm was used.

The LPCVD grown n-Ga_2O_3 on p-GaN forms a single crystalline thin film along $(\bar{2}01)$ plane denoting the β phase of Ga_2O_3 (Fig. 1(a)). The XRD pattern also shows the (0001) plane of p-GaN. Additional peaks of $Al_xGa_{(1-x)}N$ have also been observed as shown in the inset of Fig. 1(a). The surface morphology has been examined using the FESEM image (Fig. 1(b)). The cross-sectional micrographs depict the 180 nm and 500 nm thickness for Ga_2O_3 and GaN respectively along with different layers of $Al_xGa_{(1-x)}N$. Fig. 1(c) shows the XPS survey spectra of Ga_2O_3 with Ga, O and there auger states. The atomic percentage of Ga and O has been measured to be 44.13 % and 55.87 % respectively. AFM imaging for a 5 × 5 µm Ga_2O_3 layer in Fig. 1(d)

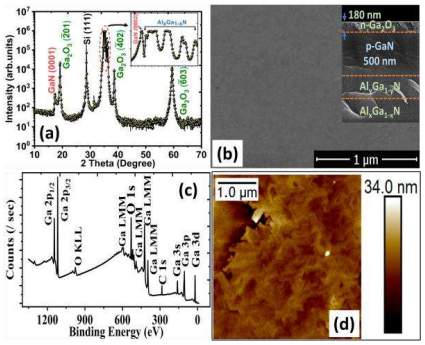

Fig. 1: (a) XRD pattern of n-Ga_2O_3/p-GaN heterostructure. The inset shows the XRD peaks of $Al_xGa_{(1-x)}N$ with different Al compositions. (b) shows the FESEM image of n-Ga_2O_3 grown on p-GaN. The inset shows the cross-sectional image with a Ga_2O_3 thickness of 180 nm. (c) XPS survey spectra of Ga_2O_3 and (d) AFM image of Ga_2O_3 showing the RMS roughness of 2.89 nm for a 5 × 5 µm layer.

AIP Publishing Applied Physics Letters ACCEPTED MANUSCRIPT
This is the author's peer reviewed, accepted manuscript. However, the online version of record will be different from this version once it has been copyedited and typeset.
PLEASE CITE THIS ARTICLE AS DOI: 10.1063/5.0215146

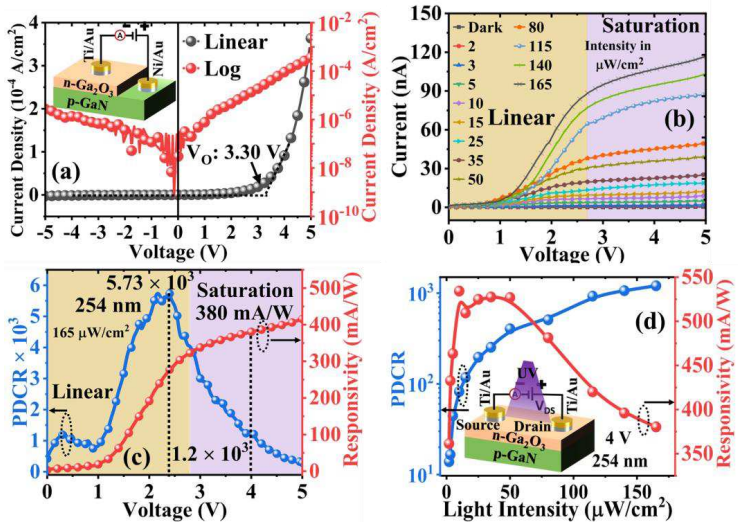

Fig. 2: (a) J-V characteristics of n-Ga_2O_3/p-GaN heterojunction diode in linear and semi-logarithmic scale with device schematic in the inset. (b) Shows the I-V characteristics of lateral n-Ga_2O_3/p-GaN based LET device in dark and illuminated conditions. The I-V characteristics have two distinct regions linear and saturation designated by yellow and purple areas respectively. Variation of PDCR and responsivity with voltage (c) and optical intensity (d) respectively for the lateral n-Ga_2O_3/p-GaN based LET device. The inset illustrates the LET device schematic.

shows a root mean square roughness of 2.89 nm. The bandgap of Ga_2O_3 deduced from the REELS has been calculated to be 4.72 eV. Fig. 2(a) shows the typical J-V characteristics of the n-Ga_2O_3/p-GaN heterojunction. When a forward bias is applied, the heterojunction shows a rectifying behavior and a high current flow after the turn-on voltage ($V_O \approx 3.30$ V). The device shows decent rectification with I_{on}/I_{off} ratio of 1.3×10^2. The low I_{on}/I_{off} ratio may be attributed to the leakage charge from the interface trap states. Montes *et al.* demonstrated mechanical exfoliated Ga_2O_3 and p-GaN heterojunction where they observed a similar high V_O of around 3.6 V [32]. The high V_O is attributed to the wide bandgap and high series resistance in Ga_2O_3. The rectification behavior of the n-Ga_2O_3/p-GaN heterojunction diode proves that a depletion region or a built-in potential (V_{bi}) exists between n-Ga_2O_3 and p-GaN. Fig. 2(b) shows the I-V characteristics of the lateral n-Ga_2O_3/p-GaN based heterojunction in dark and different illuminated intensities (2 – 165 μW/cm^2). Under dark conditions, a current of 88 pA at 4 V has been observed. When illuminated with λ~254 nm and optical intensity of 165 μW/cm^2, excess electron-hole pairs are generated which give rise to the photocurrent of 106 nA at 4 V. Further, after illumination the I-V characteristics confirm two distinct regions linear, (linear increment in photocurrent from 1 – 2.5 V) and saturation (photocurrent saturates from 2.5 – 5 V). These regions at first glance, look like the characteristics of a junction field effect transistor (JFET) first proposed by Shockley in 1952 [33]. The linear region can operate in photodetector mode and the saturation region in DM-LET mode where transistor characteristics can be used in digital and analog applications. In both operation modes, two crucial parameters need to be evaluated, photo-to-dark current ratio (*PDCR*) and responsivity (*R*) defined by equation (1) and (2) respectively.

$$PDCR = (I_{photo} - I_{dark})/I_{dark} \quad (1)$$

$$R = (I_{photo} - I_{dark})/P_O A_e \quad (2)$$

Here, I_{photo} is the photocurrent under illuminated conditions, I_{dark} is the dark current, P_O is the input power density of the light, and A_e is the effective conduction area (0.0017 cm^2). The *PDCR* and *R* are analogous to I_{on}/I_{off} ratio and transconductance respectively for an FET. Fig. 2(c) and (d) show the variation of *PDCR* and *R* with voltage (fixed optical intensity of 165 μW/cm^2) and optical intensity (fixed bias of 4 V) respectively. The behavior of *PDCR* and *R* in Fig. 2(c) is attributed to photocurrent dependence with voltage. The highest *PDCR* value of 5.73×10^3 has been observed at 2.4 V and decreased to 1.2×10^3 at 4 V for 165 μW/cm^2. At 4 V, the computed responsivity is 380 mA/W. In Fig. 2(d), the *PDCR* and *R* initially rise sharply, but the *PDCR* saturates after optical intensity of ~ 50 μW/cm^2 and the *R* decreases. The reason is attributed to the saturation of photo-

AIP Publishing Applied Physics Letters ACCEPTED MANUSCRIPT
This is the author's peer reviewed, accepted manuscript. However, the online version of record will be different from this version once it has been copyedited and typeset.
PLEASE CITE THIS ARTICLE AS DOI: 10.1063/5.0215146

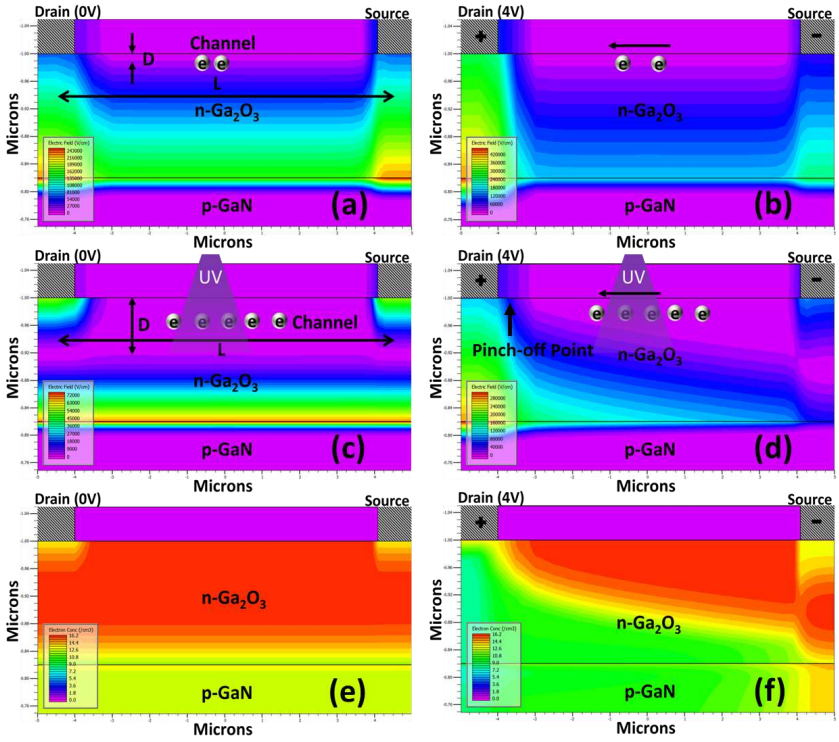

Fig. 3: Simulated electric field contour plot of n-Ga_2O_3/p-GaN heterostructure without UV illumination (a) at zero drain bias and (b) at 4 V drain bias. Simulated electric field contour plot of n-Ga_2O_3/p-GaN heterostructure under UV exposure (c) at zero drain bias and (d) at 4 V drain bias. (b) Simulated electron concentration profile of n-Ga_2O_3/p-GaN heterostructure under UV exposure (e) at zero drain bias and (f) at 4 V drain bias.

current with intensity. Experimental results also illustrate Ga_2O_3 thickness impactful for *R* and photocurrent saturation. If Ga_2O_3 thickness is low, photocurrent and correspondingly *R* is low but photocurrent saturation is strong. However, as the Ga_2O_3 thickness increases *R* increases but photocurrent saturation gets weaker.

Furthermore, Technology Computer-Aided Design (TCAD) simulations have been employed to understand the mechanism behind FET-like behavior. The simulated electric field contour plot (Fig. 3(a)) shows that the depletion region almost covers the entire Ga_2O_3 layer (180 nm), With positive voltage induced in the drain with respect to the source, current (dark current) starts to flow from drain to source through Ga_2O_3 under the influence of an electric field (Fig. 3(b)). The device's behavior becomes interesting when illuminated with UV light (1W/cm^2). Fig. 3(c) and (d) show the electric field profile of the Ga_2O_3/p-GaN heterojunction at 0 V and 4 V respectively under λ~254 nm illumination. When illuminated with λ~254 nm at a particular intensity, the Ga_2O_3 layer absorbs photons and electron-hole pairs are generated. The electron-hole pairs get quickly separated due to the built-in potential formed by the n-Ga_2O_3/p-GaN heterojunction. This phenomenon changes the overall carrier concentration in the Ga_2O_3 layer. The change in carrier concentration redistributes the depletion region in the Ga_2O_3 and a conducting channel of depth D forms as depicted in Fig. 3(c). When a small positive voltage is induced in the drain, electron starts to flow from source to drain. It should be noted at < 1 V the current is very low and can be attributed to high series resistance in Ga_2O_3. When the forward voltage becomes high (> ~ 2.5 V), pinch-off condition occurs as indicated in Fig 3(d), the channel is pinched near the drain electrode. The pinched channel resists the flow of electrons from the source to drain, resulting in current saturation. Fig. 3(e) and (f) depict the electron concentration profile along the channel at a drain voltage of 0 V and 4 V respectively. The reason behind the pinch-off condition is attributed to the reverse bias

AIP Publishing Applied Physics Letters ACCEPTED MANUSCRIPT
This is the author's peer reviewed, accepted manuscript. However, the online version of record will be different from this version once it has been copyedited and typeset.
PLEASE CITE THIS ARTICLE AS DOI: 10.1063/5.0215146

of the p-GaN. When drain becomes forward biased with respect to the source, the p-GaN becomes reversed biased. The reverse bias in a p-n heterojunction extends the depletion width towards drain side and as a result, the Ga_2O_3 channel gets pinched near the drain electrode. Higher the Ga_2O_3 thickness, carrier concentration in the channel increases and more voltage is required to pinch-off the channel. Thus, at higher Ga_2O_3 thickness the current saturation becomes weaker. Similarly, for higher doping in the Ga_2O_3, the depletion width in the Ga_2O_3 region reduces and pinch-off condition gets affected. Now, if the polarity is reversed, the source becomes forward biased and again the channel is pinched-off, however on the source side. Now, if the light power varies, the net electron density in the channel changes, modulating the channel conductivity and photocurrent. Thus, the DM-LET acts like an optically coupled JFET.

The photocurrent in a device and the incoming light power (P_{opt}) are connected by a power law given as

$$I_{ph} = AP_{opt}^{\alpha} \tag{3}$$

Here A is the proportional constant and α is the dimensionless exponent. Fig. 4(a) shows the photocurrent of the present device as a function of optical power in the saturation region (4 V). A and α have been derived to be 382 and 0.996. Almost unity α denotes trap-less photocurrent generation [34]. For a FET, an important parameter is the transconductance defined as the ratio of the change in drain current to the change in gate voltage. Larger the transconductance of a FET, greater its amplification. In FET, the current is controlled by the gate voltage but in DM-LET the optical power controls the current, so, the maximum electrical transconductance at $V_g = 0$ is given by [35]

$$g_m|_{V_g=0} \cong \frac{2I_{DS}}{V_p} \tag{4}$$

and is calculated to be 73.10 nS. Here, I_{DS} = 106 nA is the drain saturation current and V_p =2.9 V is the pinch-off voltage at λ~254 nm and 0.28 μW (165 μW/cm^2 intensity) optical power. Since, DM-LET is controlled by light intensity, a new transconductance must be defined which is a function of the photogenerated drain current and optical intensity. The optical transconductance can be defined as the ratio of the change in photogenerated drain current to the change in optical intensity and is given as

$$g_m(optical) = \frac{\delta I_{ph}}{\delta P_{opt}} = A\alpha P_{opt}^{\alpha-1} \tag{5}$$

Fig. 3(a) shows the optical transconductance in the saturation region as a function of light intensity. For an incremental change of 106 % in optical power, the $g_m(optical)$ only decreases to 0.29 %. It exhibits a decent constant $g_m(optical)$ with respect to changes in optical power. The constant $g_m(optical)$ has a vital

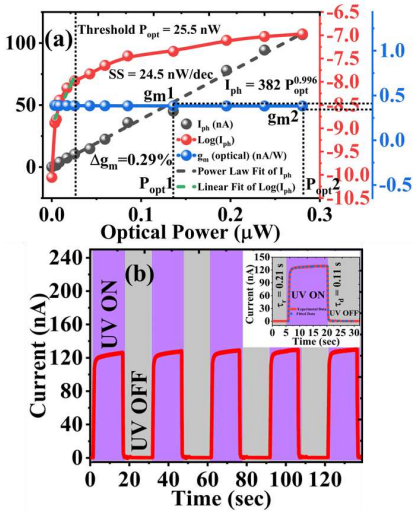

Fig. 4: (a) I_{ph}, log (I_{ph}) and g_m(optical) as a function of optical power at 4 V bias. (b) I-t response of DM-LET under 4 V bias and light intensity of 165 μW/cm^2. Inset shows the response time calculation.

significance. Considered an optical signal containing some information is fetched into an opto-electronic transducer. If the transducer has a constant $g_m(optical)$, the converted output electrical signal will be an exact replica of the input optical signal. Due to linearity, other harmonics and distortion will not be present in the output signal. Additional filtering components will then not be required in the transducer and will be cost-effective. Further, almost constant $g_m(optical)$ may also suggest minimal carrier-carrier scattering in the conduction channel. Fig. 3(a) also shows the log (I_{ph}) vs. P_{opt} curve. From the onset of the linear region of log (I_{ph}) vs. P_{opt} curve, the threshold optical power has been derived to be 25.5 nW and the inverse linear slope gives the value of the optical subthreshold swing ($SS_{optical}$) to be 24.5 nW/decade of photocurrent. The small value of the $SS_{optical}$ denotes less power required to turn on the DM-LET. The device static power consumption is also very low, with OFF and ON state power requirements of only 0.35 nW (I_{DS} = 88 pA, V_{DS} = 4 V) and 41.92 nW (I_{DS} = 10.48 nA at P_{opt} = 25.5 nW, V_{DS} = 4 V).

To demonstrate that DM-LET can act as an optically controlled switch, I-t measurements have been conducted. Fig. 4(b) shows the temporal response of the drain current for 254 at 4 V. By switching ON and OFF the UV light, the device can be turned ON or OFF. The rise time (τ_r) and fall time (τ_d) have been calculated from the exponential fitting and are given as 0.21 and 0.11 secs respectively. Table 1 compares DM-LET with state-of-the-art Ga_2O_3 based phototransistors and photodetectors showing superior performance

AIP Publishing Applied Physics Letters ACCEPTED MANUSCRIPT
This is the author's peer reviewed, accepted manuscript. However, the online version of record will be different from this version once it has been copyedited and typeset.
PLEASE CITE THIS ARTICLE AS DOI: 10.1063/5.0215146

To summarize, unique MSM DM-LET devices have been fabricated based on n-Ga_2O_3/p-GaN heterojunction. The material characteristics of n-Ga_2O_3 grown on p-GaN using LPCVD have been evaluated using XRD, FESEM, AFM and XPS. The I-V characteristics of the heterostructure device confirm transistor-like output characteristics with two separate regions linear and saturation. The two-terminal transistor structure demonstrates UV photons as the input and I_{DS} as the output. The linear region (< 2.5 V) shows photoconductivity under UV illumination and can be operated as a photodetector mode. In the saturation region (>2.5 V) the device acts as an optically controlled LET. The transistor-like behavior has been attributed to the pinch-off effect near the drain electrode due to depletion width modulation through optical excitation. TCAD simulations have been presented to confirm the pinch-off effect. Further, the device is fully controlled by the optical intensity rather than the drain voltage in the saturation region. A new parameter, optical transconductance has been calculated. The device can act as an optically controlled current source with constant optical transconductance. The device also shows a low power consumption of 0.35 nW (OFF state) and 41.92 μW (ON state) and a fast response speed (τ_r/τ_d) of 0.21/0.11 secs. Hence, the optical-electrical integration in a DM-LET permits us to use these devices in PIC and UV-NLOS communication where the conversion of optical signal into electrical signal under low power requirements is vital.

Table 1: Comparison of the parameters of reported Ga_2O_3 phototransistors and photodetector

Devices	Device Type	Driving Voltage	PDCR	R (A/W)	τ_r/τ_d (s)	Response band	FET like characteristics
Graphene/ β-Ga_2O_3	3-terminal	V_{DS}=10V V_{GS}=−8V	6×10^8	2600	1.0/0.6	254 nm	Yes [7]
β-Ga_2O_3 microflake	3-terminal	V_{DS}=6V V_{GS}=−10V	10^7	1.7×10^5	0.42/ 0.43	254 nm	Yes [10]
HfO_2/ β-Ga_2O_3	3-terminal	V_{DS}=15V V_{GS}=−27V	6.9×10^7	1.4×10^7	–	254 nm	Yes [12]
h-BN/ β-Ga_2O_3	3-terminal	V_{DS}=0.5V V_{GS}=−21V	1.52	$\approx 10^7$	0.2/3.7	254 nm	Yes [14]
β-Ga_2O_3/ p-GaN	2-terminal	0 V	4.1×10^3	3.8	0.036/ 0.073	254 – 365 nm	No [24]
β-Ga_2O_3/ GaN	2-terminal	5 V	–	3.7	–	254 – 365 nm	No [36]
β-Ga_2O_3/ p-GaN	2-terminal	12 V	–	19.2	0.1/ 0.05	240 – 370 nm	No [37]
β-Ga_2O_3/ p-GaN	**2-terminal**	**4 V**	**1.2×10^3**	**0.38**	**0.21/ 0.11**	**254 nm**	**Yes (This Work)**

See the supplementary material for the details of the XPS, band offset, REELS study, band diagrams of n-Ga_2O_3/p-GaN heterojunctions under dark and illuminated conditions, effect of thickness and doping concentration on the DM-LET device and TCAD simulation parameters.

The authors would like to acknowledge the Centre for Design and Fabrication of Electronic Devices (C4DFED) and Advanced Material Research Centre (AMRC), IIT Mandi for the characterization facilities. We would also like to acknowledge SERB (CRG/2021/006815), Indian National Academy of Engineering (INAE) (Sanction No. 2023/IN-TW/11), Department of Science and Technology (DST) and SPARC(P1456), Ministry of Human Resource and Development (MHRD), Govt. of India for funding the projects. J-I. Chyi would like to acknowledge the financial support of National Science and Technology Council of Taiwan, R.O.C. (No. NSTC 112-2923-E-008-006-MY3).

AUTHOR DECLARATION

Conflict of Interest

The authors have no conflict to disclose

DATA AVAILABILITY

The data that support the findings of this study are available upon request to the corresponding author.

REFERENCES

[1] A.K. Majumdar, "Non-Line-Of-Sight (NLOS) Ultraviolet and Indoor Free-Space Optical (FSO) Communications," (2015), pp. 177–202.
[2] C. Lin, J.S.D. Peñaranda, J. Dendooven, C. Detavernier, D. Schaubroeck, N. Boon, R. Baets, and N. Le Thomas, "UV photonic integrated circuits for far-field structured illumination autofluorescence microscopy," Nat Commun **13**(1), 4360 (2022).
[3] D.J. Blumenthal, "Photonic integration for UV to IR applications," APL Photonics **5**(2), (2020).
[4] X. Chen, F. Ren, S. Gu, and J. Ye, "Review of gallium-oxide-based solar-blind ultraviolet photodetectors," Photonics Res **7**(4), 381 (2019).
[5] A. Mondal, S. Nandi, M.K. Yadav, A. Nandi, and A. Bag, "Broad Range (254–302 nm) and High Performance Ga_2O_3:SnO_2 Based

AIP Publishing Applied Physics Letters ACCEPTED MANUSCRIPT
This is the author's peer reviewed, accepted manuscript. However, the online version of record will be different from this version once it has been copyedited and typeset.
PLEASE CITE THIS ARTICLE AS DOI: 10.1063/5.0215146

Deep UV Photodetector," IEEE Trans Nanotechnolgy **21**, 320–327 (2022).
[6] D. Kaur, and M. Kumar, "A Strategic Review on Gallium Oxide Based Deep-Ultraviolet Photodetectors: Recent Progress and Future Prospects," Adv Opt Mater **9**(9), 2002160 (2021).
[7] S. Kim, S. Oh, and J. Kim, "Ultrahigh Deep-UV Sensitivity in Graphene-Gated β-Ga_2O_3 Phototransistors," ACS Photonics **6**(4), 1026–1032 (2019).
[8] J. Ahn, J. Ma, D. Lee, Q. Lin, Y. Park, O. Lee, S. Sim, K. Lee, G. Yoo, and J. Heo, "Ultrahigh Deep-Ultraviolet Responsivity of a β-Ga_2O_3/MgO Heterostructure-Based Phototransistor," ACS Photonics **8**(2), 557–566 (2021).
[9] P. Tan, Y. Zou, X. Zhao, X. Hou, Z. Zhang, M. Ding, S. Yu, X. Ma, G. Xu, Q. Hu, and S. Long, "Hysteresis-free Ga_2O_3 solar-blind phototransistor modulated from photoconduction to photogating effect," Appl Phys Lett **120**(7), 071106 (2022).
[10] S. Yu, X. Zhao, M. Ding, P. Tan, X. Hou, Z. Zhang, W. Mu, Z. Jia, X. Tao, G. Xu, and S. Long, "High-Detectivity *β*-Ga_2O_3 Microflake Solar-Blind Phototransistor for Weak Light Detection," IEEE Electron Device Letters **42**(3), 383–386 (2021).
[11] X.-X. Li, G. Zeng, Y.-C. Li, H. Zhang, Z.-G. Ji, Y.-G. Yang, M. Luo, W.-D. Hu, D.W. Zhang, and H.-L. Lu, "High responsivity and flexible deep-UV phototransistor based on Ta-doped β-Ga_2O_3," Npj Flexible Electronics **6**(1), 47 (2022).
[12] Z. Li, Z. Feng, Y. Xu, Q. Feng, W. Zhu, D. Chen, H. Zhou, J. Zhang, C. Zhang, and Y. Hao, "High Performance β-Ga_2O_3 Solar-Blind Metal–Oxide–Semiconductor Field-Effect Phototransistor With Hafnium Oxide Gate Dielectric Process," IEEE Electron Device Letters **42**(4), 545–548 (2021).
[13] Y. Xu, Y. Cheng, Z. Li, Q. Feng, Y. Zhang, D. Chen, W. Zhu, J. Zhang, C. Zhang, and Y. Hao, "High performance gate tunable solar blind ultraviolet phototransistors based on amorphous Ga_2O_3 films grown by mist chemical vapor deposition," Nano Select **2**(11), 2112–2120 (2021).
[14] X.-X. Li, G. Zeng, Y.-C. Li, Q.-J. Yu, M.-Y. Liu, L.-Y. Zhu, W. Liu, Y.-G. Yang, D.W. Zhang, and H.-L. Lu, "Highly sensitive and stable β-Ga_2O_3 DUV phototransistor with local back-gate structure and its neuromorphic application," Nano Res **15**(10), 9359–9367 (2022).
[15] X. Ji, Y. Yuan, X. Yin, S. Yan, Z. Ding, J. Zhang, Q. Xin, and A. Song, "Amorphous Ga_2O_3 Thin-Film Phototransistors for Imaging and Logic Illustration," IEEE Electron Device Letters, 1–1 (2023).
[16] Y. Li, C. Deng, B. Huang, S. Yang, J. Xu, G. Zhang, S. Hu, D. Wang, B. Liu, Z. Ji, L. Lan, and J. Peng, "High-Performance Solar-Blind UV Phototransistors Based on ZnO/Ga_2O_3 Heterojunction Channels," ACS Appl Mater Interfaces **15**(14), 18372–18378 (2023).
[17] Y. Yoon, W.S. Hwang, and M. Shin, "Solar-Blind Ultrathin Sn-Doped Polycrystalline Ga_2O_3 UV Phototransistor for Normally Off Operation," Adv Photonics Res **3**(5), 2100316 (2022).
[18] H.T. Ng, J. Han, T. Yamada, P. Nguyen, Y.P. Chen, and M. Meyyappan, "Single Crystal Nanowire Vertical Surround-Gate Field-Effect Transistor," Nano Lett **4**(7), 1247–1252 (2004).
[19] T. Shinada, S. Okamoto, T. Kobayashi, and I. Ohdomari, "Enhancing semiconductor device performance using ordered dopant arrays," Nature **437**(7062), 1128–1131 (2005).
[20] J.K. Marmon, S.C. Rai, K. Wang, W. Zhou, and Y. Zhang, "Light-Effect Transistor (LET) with Multiple Independent Gating Controls for Optical Logic Gates and Optical Amplification," Front Phys **4**, (2016).
[21] A. Kumar, A. Nandi, and A. Bag, "Exceptional Responsivity (6 kA/W) and Dark Current (70 fA) Tradeoff of n-Ga_2O_3/p-CuO Quasi-Heterojunction-Based Deep UV Photodetector," IEEE Trans Electron Devices **68**(1), 144–151 (2021).
[22] D. Guo, Y. Su, H. Shi, P. Li, N. Zhao, J. Ye, S. Wang, A. Liu, Z. Chen, C. Li, and W. Tang, "Self-Powered Ultraviolet Photodetector with Superhigh Photoresponsivity (3.05 A/W) Based on the GaN/Sn:Ga_2O_3 pn Junction," ACS Nano **12**(12), 12827–12835 (2018).
[23] X.C. Guo, N.H. Hao, D.Y. Guo, Z.P. Wu, Y.H. An, X.L. Chu, L.H. Li, P.G. Li, M. Lei, and W.H. Tang, "β-Ga_2O_3/p-Si heterojunction solar-blind ultraviolet photodetector with enhanced photoelectric responsivity," J Alloys Compd **660**, 136–140 (2016).
[24] Y. Ma, T. Chen, X. Zhang, W. Tang, B. Feng, Y. Hu, L. Zhang, X. Zhou, X. Wei, K. Xu, D. Mudiyanselage, H. Fu, and B. Zhang, "High-Photoresponsivity Self-Powered *a* -, ε-, and β-Ga_2O_3/p-GaN Heterojunction UV Photodetectors with an *In Situ* GaON Layer by MOCVD," ACS Appl Mater Interfaces **14**(30), 35194–35204 (2022).
[25] J. Wang, X. Ji, Z. Yan, X. Yan, C. Lu, Z. Li, S. Qi, S. Li, X. Qi, S. Zhang, S. Hu, and P. Li, "High sensitivity Ga_2O_3 ultraviolet photodetector by one-step thermal oxidation of p-GaN films," Mater Sci Semicond Process **159**, 107372 (2023).
[26] P.-F. Chi, F.-W. Lin, M.-L. Lee, and J.-K. Sheu, "High-Responsivity Solar-Blind Photodetectors Formed by Ga_2O_3/p-GaN Bipolar Heterojunctions," ACS Photonics **9**(3), 1002–1007 (2022).
[27] K. Tetzner, K. Egbo, M. Klupsch, R.-S. Unger, A. Popp, T.-S. Chou, S. Bin Anooz, Z. Galazka, A. Trampert, O. Bierwagen, and J. Würfl, "SnO/β-Ga_2O_3 heterojunction field-effect transistors and vertical p–n diodes," Appl Phys Lett **120**(11), 112110 (2022).
[28] C. Li, C. Chen, J. Chen, T. He, H. Li, Z. Yang, L. Xie, Z. Wang, and K. Zhang, "High-performance junction field-effect transistor based on black phosphorus/β-Ga_2O_3 heterostructure," Journal of Semiconductors **41**(8), 082002 (2020).
[29] J. Kim, M.A. Mastro, M.J. Tadjer, and J. Kim, "Heterostructure WSe_2–Ga_2O_3 Junction Field-Effect Transistor for Low-Dimensional High-Power Electronics," ACS Appl Mater Interfaces **10**(35), 29724–29729 (2018).
[30] A. Mondal, M.K. Yadav, and A. Bag, "Transition from thin film to nanostructure in low pressure chemical vapor deposition growth of β-Ga_2O_3: Impact of metal gallium source," Thin Solid Films **709**, 138234 (2020).
[31] I. Sanyal, Y.-C. Lee, Y.-C. Chen, and J.-I. Chyi, "Achieving high electron mobility in AlInGaN/GaN heterostructures: The correlation between thermodynamic stability and electron transport properties," Appl Phys Lett **114**(22), (2019).
[32] J. Montes, C. Yang, H. Fu, T.-H. Yang, K. Fu, H. Chen, J. Zhou, X. Huang, and Y. Zhao, "Demonstration of mechanically exfoliated *β*-Ga_2O_3/GaN p-n heterojunction," Appl Phys Lett **114**(16), 162103 (2019).
[33] W. Shockley, "A Unipolar 'Field-Effect' Transistor," Proceedings of the IRE **40**(11), 1365–1376 (1952).
[34] Q. Zhao, W. Wang, F. Carrascoso-Plana, W. Jie, T. Wang, A. Castellanos-Gomez, and R. Frisenda, "The role of traps in the photocurrent generation mechanism in thin InSe photodetectors," Mater Horiz **7**(1), 252–262 (2020).
[35] B.G. Streetman, and S.K. Banerjee, *Solid State Electronic Devices*, Seventh Edition, Pearson Education Limited, p. 286-287, (2016).
[36] A. Kalra, S. Vura, S. Rathkanthiwar, R. Muralidharan, S. Raghavan, and D.N. Nath, "Demonstration of high-responsivity epitaxial β-Ga_2O_3/GaN metal–heterojunction-metal broadband UV-A/UV-C detector," Applied Physics Express **11**(6), 064101 (2018).
[37] R. Tang, G. Li, Y. Jiang, N. Gao, J. Li, C. Li, K. Huang, J. Kang, T. Wang, and R. Zhang, "Ga_2O_3/GaN Heterostructural Ultraviolet Photodetectors with Exciton-Dominated Ultranarrow Response," ACS Appl Electron Mater **4**(1), 188–196 (2022).